jmb Article

Glycan Shifting on Hepatitis C Virus (HCV) E2 Glycoprotein Is a Mechanism for Escape from Broadly Neutralizing Antibodies

Homer Pantua[1]†, Jingyu Diao[1]†, Mark Ultsch[2], Meredith Hazen[3], Mary Mathieu[3], Krista McCutcheon[3], Kentaro Takeda[4], Shailesh Date[5], Tommy K. Cheung[4], Qui Phung[4], Phil Hass[4], David Arnott[4], Jo-Anne Hongo[3], David J. Matthews[6], Alex Brown[6], Arvind H. Patel[7], Robert F. Kelley[3], Charles Eigenbrot[2,3] and Sharookh B. Kapadia[1]

*1 - **Department of Infectious Diseases,** Genentech, 1 DNA Way, South San Francisco, CA 94080, USA*
*2 - **Department of Structural Biology,** Genentech, 1 DNA Way, South San Francisco, CA 94080, USA*
*3 - **Department of Antibody Engineering,** Genentech, 1 DNA Way, South San Francisco, CA 94080, USA*
*4 - **Department of Protein Chemistry,** Genentech, 1 DNA Way, South San Francisco, CA 94080, USA*
*5 - **Department of Bioinformatics,** Genentech, 1 DNA Way, South San Francisco, CA 94080, USA*
*6 - **Therapeutic Antibody Group,** MRC Technology, London NW7 1AD, UK*
*7 - **MRC–University of Glasgow Centre for Virus Research,** Glasgow G11 5JR, UK*

***Correspondence to Charles Eigenbrot and Sharookh B. Kapadia:** C. Eigenbrot is to be contacted at Department of Structural Biology, Genentech, 1 DNA Way, South San Francisco, CA 94080, USA; S. B. Kapadia, Department of Infectious Diseases, Genentech, 1 DNA Way, South San Francisco, CA 94080, USA. eigenbrot.c@gene.com; kapadia.sharookh@gene.com*
http://dx.doi.org/10.1016/j.jmb.2013.02.025
Edited by I. Wilson

Abstract

Hepatitis C virus (HCV) infection is a major cause of liver disease and hepatocellular carcinoma. Glycan shielding has been proposed to be a mechanism by which HCV masks broadly neutralizing epitopes on its viral glycoproteins. However, the role of altered glycosylation in HCV resistance to broadly neutralizing antibodies is not fully understood. Here, we have generated potent HCV neutralizing antibodies hu5B3.v3 and MRCT10.v362 that, similar to the previously described AP33 and HCV1, bind to a highly conserved linear epitope on E2. We utilize a combination of *in vitro* resistance selections using the cell culture infectious HCV and structural analyses to identify mechanisms of HCV resistance to hu5B3.v3 and MRCT10.v362. Ultra deep sequencing from *in vitro* HCV resistance selection studies identified resistance mutations at asparagine N417 (N417S, N417T and N417G) as early as 5 days post treatment. Comparison of the glycosylation status of soluble versions of the E2 glycoprotein containing the respective resistance mutations revealed a glycosylation shift from N417 to N415 in the N417S and N417T E2 proteins. The N417G E2 variant was glycosylated neither at residue 415 nor at residue 417 and remained sensitive to MRCT10.v362. Structural analyses of the E2 epitope bound to hu5B3.v3 Fab and MRCT10.v362 Fab using X-ray crystallography confirmed that residue N415 is buried within the antibody–peptide interface. Thus, in addition to previously described mutations at N415 that abrogate the β-hairpin structure of this E2 linear epitope, we identify a second escape mechanism, termed glycan shifting, that decreases the efficacy of broadly neutralizing HCV antibodies.

Introduction

Hepatitis C virus (HCV), a member of the *Flaviviridae* family of viruses, is a major cause of chronic hepatitis and hepatocellular carcinoma.[1,2] The HCV genome is a positive-strand, ~9.6-kb RNA molecule consisting of a single open reading frame flanked by 5′ and 3′ untranslated regions (UTRs). The HCV 5′ UTR contains a highly structured internal ribosome entry site[2–6] while the 3′ UTR is essential for replication.[7–9] The HCV open reading frame encodes a single polyprotein of ~3000 amino acids in length and is posttranslationally processed to produce at least 10 different proteins: core, envelope

proteins E1 and E2, p7 and non-structural proteins NS2, NS3, NS4A, NS4B, NS5A and NS5B.[1,10,11]

HCV entry into hepatocytes occurs through the coordinated interactions between the HCV E1–E2 heterodimer and at least four essential cellular factors: CD81,[12] scavenger receptor B type I,[13] occludin[14,15] and claudin 1 (CLDN1).[16] In particular, the HCV E2 glycoprotein binds CD81 and scavenger receptor B type I, and anti-HCV E2 neutralizing antibodies, especially ones that bind to a highly conserved epitope on E2 ($E2^{412–423}$), are broadly neutralizing across multiple HCV genotypes.[17–22] The extracellular domains of both E1 and E2 are heavily glycosylated, and some glycans are critical for viral infectivity *in vitro*.[23] HCV resistance to neutralizing antibodies can arise from the high mutational rate of the HCV polymerase ($\sim 10^{-4}$ per nucleotide per generation), shielding of the E1–E2 glycoproteins by virion-associated lipoproteins or the presence of non-neutralizing antibodies that prevent binding of neutralizing antibodies.[24] Recent studies have revealed the importance of glycosylated asparagine (Asn) residues in E2 in the masking of epitopes recognized by broadly neutralizing antibodies.[23,25,26] Multiple glycans on E2, including those on N417 and N423 (termed E2N1 and E2N2 in the literature), decrease sensitivity of infectious cell culture HCV (HCVcc) and HCV pseudoparticles (HCVpp) to neutralization by patient antisera and modulate binding of a soluble form of CD81, suggesting that glycans play an important role in masking the CD81 binding epitope on E2.[25–27] However, many of these mutational analyses have involved substitutions with alanine[25] or glutamine[23] residues and it is unclear whether viruses bearing these changes are competent for viral entry. Although Dhillon *et al.* have demonstrated that virus isolates containing mutations at N415 and N417 confer resistance to the murine monoclonal antibody AP33,[28] the mechanisms of resistance were not clear.

Recently, using crystal structures of two other $E2^{412–423}$-specific neutralizing antibodies, HCV1 and AP33, complexed with its peptide epitope, Kong *et al.* and Potter *et al.* have demonstrated that mutations at N415 can result in loss of HCV neutralization as this residue is within the antibody–peptide interface.[29–31] In this report, we identify N417S and N417T HCVcc variants that are resistant to two broadly neutralizing affinity-matured antibodies, MRCT10.v362 and hu5B3.v3, and conclude that a glycosylation shift from residue N417 to N415 causes this resistance. Furthermore, in spite of the emergence of robust resistance of the N417S HCVcc variant, combination with an approved HCV direct acting antiviral (DAA) resulted in significant suppression of resistance to both HCV DAA and MRCT10.v362. Cumulatively, our data demonstrate that shifts in the glycan attachment site within the CD81 binding epitope on E2 play a critical role in conferring resistance to neutralizing antibodies and that combining viral entry inhibitors with HCV antivirals with an orthogonal mechanism of action can enhance the antiviral effect and suppress emergence of these resistant variants.

Results

Rapid and robust HCV genotype-specific resistance develops to $E2^{412–423}$-specific neutralizing antibodies *in vitro*

The humanization and affinity maturation of the murine antibodies AP33 and mu5B3 to generate MRCT10.v362 and hu5B3.v3, respectively, are described in detail in Supplemental Materials. MRCT10.v362 and hu5B3.v3 had ~2-fold increased binding affinity to soluble versions of E2 ($sE2_{661}$) from both genotype 1a and genotype 1b relative to the parental antibodies as shown by surface plasmon resonance (SPR) analysis (Table S2). The affinity improvements resulted primarily from a decreased off-rate. Kinetics of binding were slower for hu5B3.v3 compared to MRCT10.v362. In comparison, both affinity-matured variants hu5B3.v3 and MRCT10.v362 had significantly improved *in vitro* neutralization potencies compared to their parental murine antibodies, mu5B3 and AP33, against both HCVpp (Table 1) and wild-type genotype 2a Jc1

Table 1. HCVpp neutralization of affinity-matured $E2^{412–423}$-specific antibodies

	HCVpp neutralization (EC_{90}, μg/mL)		
Antibodies	GT1a (H77)	GT1b (Con1)	GT2a (J6CF)
AP33	0.34 ± 0.013	6.86 ± 1.27	7.94 ± 2.45
MRCT10.v362	0.07 ± 0.02	2 ± 0.11	1.76 ± 0.4
mu5B3	0.52 ± 0.14	44.7 ± 15.73	107.7 ± 22.32
hu5B3.v3	0.73 ± 0.62	9.22 ± 4.3	17.48 ± 9.46
HCV1	4.81 ± 2.28	93.4 ± 35.29	72.3 ± 7.79
Anti-CD81	0.35 ± 0.085	0.286 ± 0.22	0.15 ± 0.05
Anti-CLDN1	7.38 ± 0.75	6.45 ± 2.58	3.84 ± 1.74

All values represent averages ± SEM and are representative of at least two independent experiments each performed in triplicate. Average EC_{90} values for mu5B3 and hu5B3.v3 were generated from at four independent experiments.

Table 2. Effect of mutations identified in Jc1 $E2^{412–423}$ on Jc1 HCVcc sensitivity to HCV antibodies and antivirals

	EC_{90} of Jc1 HCVcc variants to HCV antivirals (μg/mL)				
	N417 (WT)	N417S	N417T	N417G	N415D
AP33	4.6 ± 0.95[a]	>100[a]	>100	9.7 ± 5.1	>100
MRCT10.v362	0.58 ± 0.27[a]	>100[a]	>100	1.23 ± 0.26	>100
mu5B3	5.1 ± 2.9	>100	>100	24.5 ± 12.9	>100
hu5B3.v3	0.66 ± 0.32	>100	>100	7.1 ± 0.98	>100
HCV1	2.3 ± 0.36	>100	>100	42 ± 3.8	>100
Anti-CD81	0.089 ± 0.06	0.023 ± 0.003	0.032 ± 0.005	0.032 ± 0.018	0.032 ± 0.006
Anti-CLDN1	0.18 ± 0.003[a]	0.263 ± 0.1[a]	0.174 ± 0.032[a]	0.22 ± 0.13[a]	0.54 ± 0.15[a]

All values represent averages ± SEM and are representative of at least two independent experiments each performed in triplicate.
[a] Values are determined from three independent experiments.

HCVcc (Table 2). Subsequent binding studies using the $E2^{412–423}$ peptide demonstrated that mu5B3 bound to a similar overlapping peptide as AP33 (data not shown).

Since hu5B3.v3 and MRCT10.v362 bound a similar epitope on E2, we wanted to determine whether mutations that conferred AP33 resistance in Jc1 (chimeric genotype 2a) and Con1/C3-neo (chimeric genotype 1b) HCVcc would also lead to resistance against hu5B3.v3. To identify mutations conferring resistance to AP33, we selected for resistant isolates by gradually increasing the antibody concentration in two ways. The first involved sequential passaging of supernatants from infected cells onto uninfected cells to identify dominant resistant isolates (Fig. 1a). The second involves continuous passaging of infected cells in order to allow for the assembly and release of variants that may be attenuated in growth and spread (Fig. 1a). Incubation of genotype 2a Jc1 HCVcc with increasing concentrations of AP33 resulted in an initial ~10-fold decrease in HCV RNA replication followed by a rapid rebound in HCV RNA replication as early as 10 days post infection (Fig. 1b). Within 2 weeks, the levels of HCV RNA replication were similar to that of cultures not treated with antibody (Fig. 1b). In comparison, no resistant virus could be detected by passaging supernatants from genotype 1b chimeric Con1/C3 HCVcc-infected Huh7.5 cells (Fig. 1b). Culturing in the presence of a control antibody did not lead to a decrease in HCV RNA replication and spread (data not shown).

Bulk sequencing and single genome sequencing using primers surrounding the $E2^{412–423}$ epitope revealed single point mutations at residues 417 (N417S) and 415 (N415D) in the continuous Jc1 HCVcc supernatant and cell passaging experiments, respectively. While no dominant mutations were detected in the Con1/C3 supernatant passage experiment, the N415D mutation was detected in continuously passaged Con1/C3 HCVcc-infected cells by single genome sequencing (data not shown). To further determine if additional subdominant resistance mutations exist and to understand the kinetics of the emergence of these mutations, we performed 454 ultra deep sequencing analysis of Jc1 HCVcc-infected cells at various times post infection and determined the frequency of amino acids at positions 415 and 417. Between 16,000 and 25,000 reads per treatment per time point were analyzed. In the absence of any selecting antibody, the wild-type N415 (data not shown) and N417 (Fig. 1c) sequences were the dominant species (>94%) in the culture at all time points tested. No enrichment of N415 variants was detected in the supernatant passed cultures (data not shown). However, compared to untreated cells, incubation with AP33 resulted in a 39-fold (8.5% *versus* 0.2%) and 138-fold (23.4% *versus* 0.17%) enrichment of Jc1 HCVcc genomes containing N417S and N417T mutations, respectively, as early as 5 days post selection (Fig. 1c). By 15 days post infection, the N417S HCVcc variant had become the dominant species (Fig. 1c). N417G Jc1 HCVcc variants were detected but not enriched in antibody-treated infections.

N417S and N417T Jc1 HCVcc are resistant to hu5B3.V3 and MRCT10.v362 neutralization

In order to determine whether N417S, N417T, N417G and N415D mutations conferred resistance to $E2^{412–423}$-specific neutralizing antibodies, we independently introduced each of these mutations into Jc1 HCVcc and tested the ability of various antibodies to inhibit entry and infection. AP33 and HCV1 antibodies were used as controls. As expected, the N417S, N417T and N415D HCVcc were completely resistant to inhibition by all $E2^{412–423}$-specific neutralizing antibodies AP33, MRCT10.v362, mu5B3, hu5B3.v3 and HCV1 (Table 2). In comparison, all HCVcc variants were equivalently sensitive to anti-CD81 and anti-CLDN1 neutralizing antibodies (Table 2). Interestingly, while both wild-type and N417G HCVcc remained equivalently sensitive to AP33 and MRCT10.v362, the N417G variant was more resistant to mu5B3, hu5B3.v3 and HCV1 (~5-fold, 11-fold and 18-fold, respectively). The lack of enrichment of the N417T

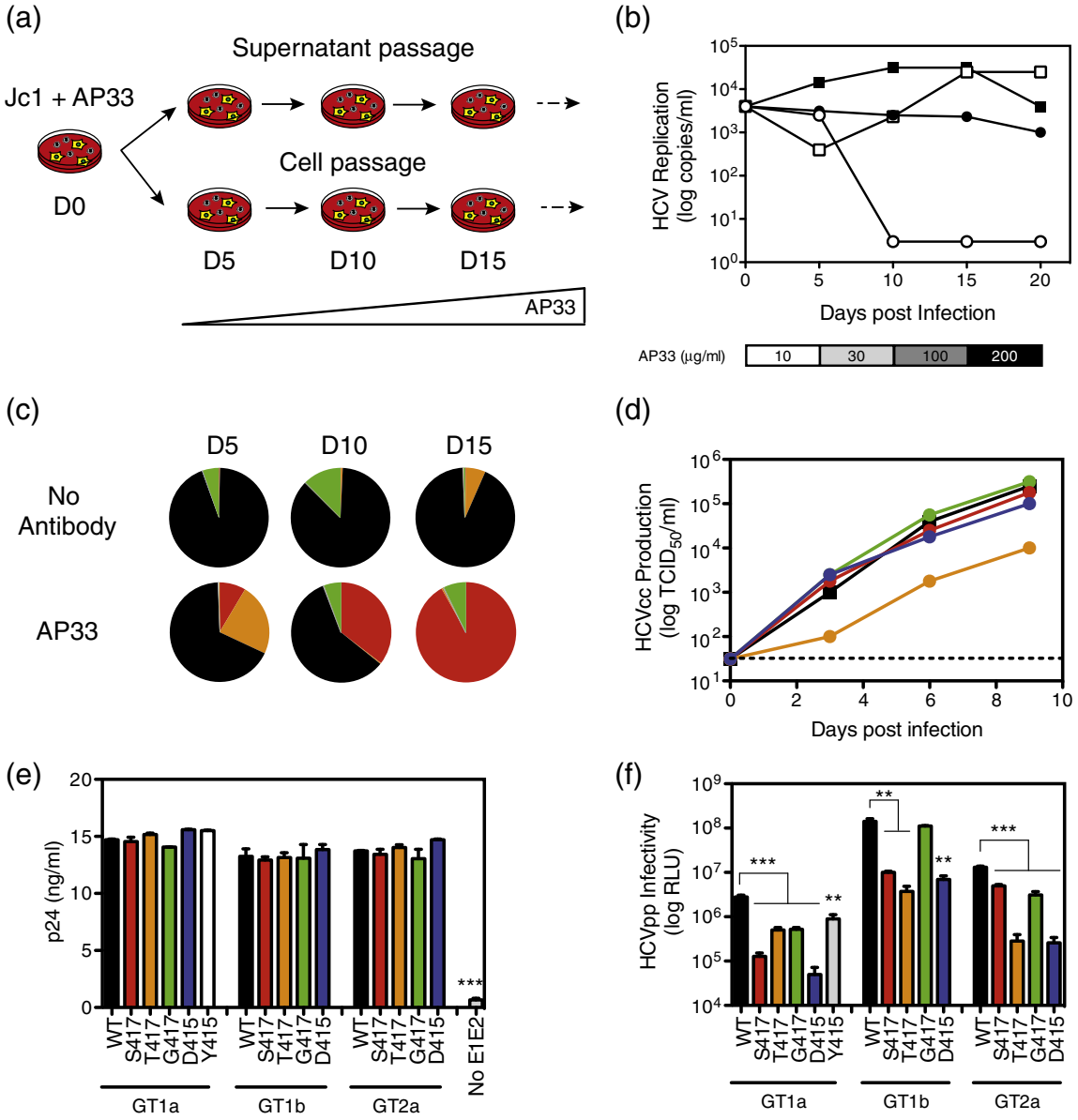

Fig. 1. Identification and characterization of mutant Jc1 and Con1/C3-neo HCVcc resistant to E2$^{412–423}$-specific neutralizing antibody (AP33). (a) Supernatants and cells from Jc1 (squares) and Con1/C3-neo (circles) HCVcc-infected Huh7.5 cells were sequentially cultured in the absence (filled symbols) or presence (open symbols) of increasing concentrations of AP33, and (b) HCV RNA replication was measured at various times post infection. These are representative data from three independent experiments. (c) 454 Ultra deep sequencing analysis of N417 amino acid variations over time demonstrating an enrichment of the N417S mutant HCVcc when cultured in the presence of antibody (WT, black; N417S, red; N417T, orange; N417G, green). (d) The effect of the mutations on HCVcc infectivity was determined by introducing them in Jc1 HCVcc and monitoring growth in culture over 9 days. (e and f) The effect of the identified mutations on infectivity of HCVpp was determined. HCVpp stocks were generated and normalized using p24 levels in the supernatants (e) followed by infecting Huh7.5 cells to measure infectivity (f). No pseudoparticles were generated in the absence of E1E2-expressing plasmid as determined by p24 levels. *In vitro* growth and infectivity studies are representative data from at least two independent experiments. *p* values: $*p < 0.05$, $**p < 0.01$ and $***p < 0.001$.

HCVcc in the *in vitro* resistance selection is likely due to its ≥10-fold decreased infectivity *in vitro* (Fig. 1d).

Since no resistant mutations were detected using the genotype 1b chimeric virus Con1/C3-neo, we wanted to determine whether the resistance mutations, when present in genotype 1 HCV, resulted in decreased infectivity. The N415 and N417 mutations were introduced into H77, Con1 and J6CF E1E2-expressing plasmids by site-directed mutagenesis and HCVpp stocks were generated. As a control, we

introduced the N415Y mutation into genotype 1a E2 that has been previously demonstrated to confer resistance to AP33.[32] Equivalent levels of each HCVpp variant were generated as measured by p24 levels in the supernatant after co-transfection with the lentiviral vectors. No p24 was detected in the absence of co-transfection of E1E2-expressing plasmid (Fig. 1e). While N417S HCVpp infectivity was only modestly decreased (~2.6-fold) compared to that of wild-type HCVpp from genotype 2a J6CF (Fig. 1f), introduction of N417S resulted in significantly decreased entry of genotypes 1b and 1a HCVpp (~14-fold and ~22-fold, respectively). In comparison, the infection of N417T and N415D HCVpp were significantly decreased in all HCVpp genotypes tested (Fig. 1f). The N415Y genotype 1a HCVpp was modestly attenuated compared to wild-type H77 HCVpp, similar to what has been previously described.[32]

Loss of hu5B3.V3 and MRCT10.v362 binding to N417S and N417T E2 glycoproteins expressed in mammalian cells

We compared binding of hu5B3.V3 and MRCT10.v362 to either $E2^{412–423}$ peptide or full-length E1E2

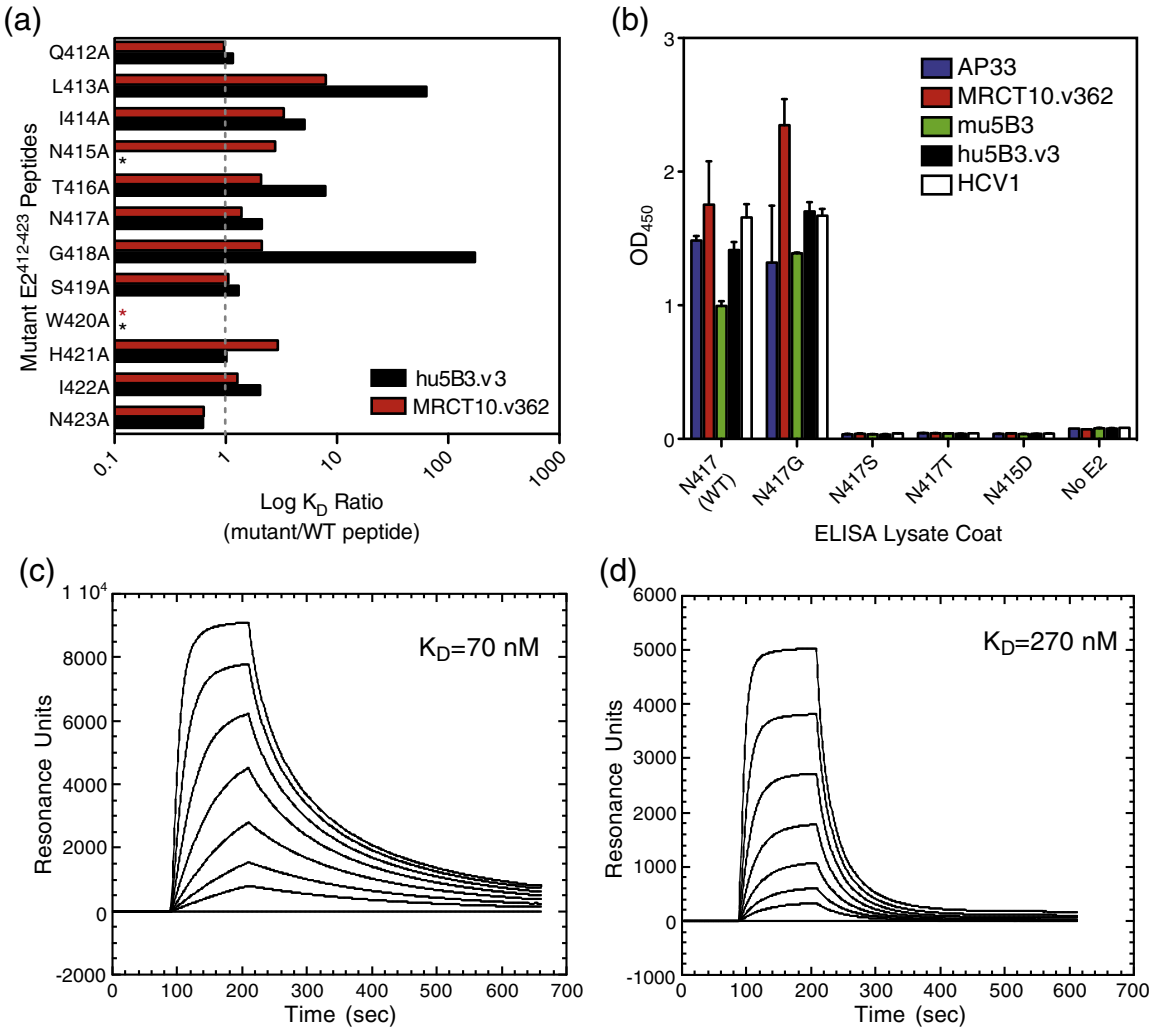

Fig. 2. Binding of hu5B3.v3 and MRCT10.v362 to wild-type and mutant soluble E2 proteins ($sE2_{661}$) and $E2^{412–423}$ peptides. (a) Ratio of dissociation constants (K_D) for MRCT10.v362 (red) and hu5B3.v3 (black) binding to alanine mutant peptides relative to WT peptide QLINTNGSWHINGSGK-biotin ($E2^{412–423\text{-biotin}}$) are graphed. Asterisks denote no binding detected with mutant peptides. (b) Binding of various $E2^{412–423}$-specific neutralizing antibodies to lysates of untransfected 293 cells (No E2) or 293 cells transfected with genotype 2a (J6CF) HCV E1E2-expressing plasmids containing various mutations at N415 or N417. These are representative data from three independent experiments. (c and d) MRCT10 Fab binds to N417S $E2^{412–423}$. Biacore sensorgrams demonstrating binding of MRCT10 Fab to WT (c) or N417S (d) $E2^{412–423}$ peptide. The Fab series was diluted 2-fold starting from 1000 nM down to 15.6 nM. MRCT10 Fab binds to N417S $E2^{412–423}$ peptide with faster off-rate compared to WT. Dissociation constants (K_D) are listed in the graphs.

expressed in transfected cells. Binding of Fab fragments to chemically synthesized peptides (non-glycosylated) was measured by SPR or bio-layer interferometry. Both MRCT10.v362 and hu5B3.v3 showed measurable binding affinity to the $E2^{412–423}$ peptide epitope with K_D values of 30 nM and 12 nM, respectively (data not shown). Binding studies using alanine mutations of the peptide demonstrated some similarities for the two antibodies (Fig. 2a). While both MRCT10.v362 and hu5B3.v3 did not bind W420A mutant peptide, they bound both wild-type and N417A mutant peptides equivalently (Fig. 2a). In comparison, while mutants L413A and G418A exhibited ~64-fold and ~174-fold decreases in binding affinity for hu5B3.v3, respectively, they only affected MRCT10.v362 binding by ~8-fold and ~2-fold, respectively (Fig. 2a). In addition, while binding of MRCT10.v362 to N415A only decreased by 2.8-fold, binding of hu5B3.v3 was completely lost (Fig. 2a). These data suggest that both MRCT10.v362 and hu5B3.v3 bind similar epitopes through different interactions.

Since the region surrounding the $E2^{412–423}$ epitope is highly glycosylated on virion-associated E2, we wanted to determine whether these posttranslational modifications would affect binding of hu5B3.v3 or MRCT10.v362. In order to determine if hu5B3.v3 and MRCT10.v362 bound recombinant E2 containing the N417S or N417T mutations, we tested antibody binding to a soluble E2 glycoprotein variant ($sE2_{661}$) or E1E2 expressed in cells using SPR and ELISA, respectively. SPR measurements indicated that affinity of hu5B3.v3 and MRCT10.v362 for N417S and N417T $sE2_{661}$ was reduced at least 100-fold ($K_D > 500$ nM) whereas binding of N417G $sE2_{661}$ was decreased only 3-fold (data not shown). Furthermore, hu5B3.v3 and MRCT10.v362 binding to E1E2-expressing 293T cell lysates demonstrated no detectable binding to N417S, N417T or N415D with any of the $E2^{412–423}$-specific antibodies (Fig. 2b). Interestingly, MRCT10 Fab still bound the N417S peptide, although with ~3.9-fold less affinity compared to the wild-type peptide (Fig. 2c and d). These data are consistent with the hypothesis that posttranslational modifications on the native N417S or N417T E2 protein in the $E2^{412–423}$ epitope may prevent antibody binding.

N415 is glycosylated in the N417S and N417T mutant E2 proteins

Identifying glycosylated Asn residues on E2 derived from intact HCVcc particles is technically challenging. Since $sE2_{661}$ has been demonstrated to retain many aspects of the E2 glycoprotein including CD81 binding, we determined the glycosylation status of Asn residues within the $E2^{412–423}$ epitope in $sE2_{661}$ proteins secreted by Huh7.5 cells, as these are the same cells used for HCVcc infection and virus production *in vitro*. Huh7.5 cells were transfected with plasmids expressing recombinant J6CF $sE2_{661}$ variants containing N417 (WT), S417, T417 or G417 mutations. The $sE2_{661}$ proteins were purified and asparagine glycosylation state within the $E2^{412–423}$ epitope was characterized by mass spectrometry (MS), as performed previously.[33] Concordant with previously published results,[33] wild-type $sE2_{661}$ was glycosylated at both N417 and N423 (Fig. S2a). Not surprisingly, while both N417S and N417T $sE2_{661}$ were glycosylated at N415 and N423 (Fig. S2b and c), the N417G $sE2_{661}$ was only glycosylated at N423 (Fig. S2d). Since N417G Jc1 HCVcc was not attenuated *in vitro* and both wild-type and N417G HCVcc remained equivalently sensitive to MRCT10.v362 neutralization, our data suggest that the glycosylation shift from residue 417 to residue N415 may be important for generating

Table 3. H-bonds within the E2 peptide (Å) for MRCT1.v362 and hu5B3.v3 compared to other $E2^{412–423}$-specific antibody–peptide structures

Atom 1	Atom 2	5B3	v362 chain Z	v362 chain Y	HCV1 PDB 4GDV	HCV1 PDB 4GDY	AP33 PDB 4GAG	AP33 PDB 4GAJ
Q412 O	N423 N	3.2	—[a]	—	2.9	2.9	b	—
I414 N	H421 O	2.9	2.9	2.9	2.8	2.7	2.8	3.0
I414 O	H241 N	3.0	2.9	2.8	2.9	2.9	2.9	2.9
N415 Oδ1	G418 N	2.9	3.1	3.1	2.8	3.0	3.1	2.9
N415 Oδ1	S419 N	3.1	—	—	—	—	—	—
T416 N	S419 O	—	3.0	3.0	2.9	2.9	2.9	3.1
T416 O	S419 N	—	3.1	3.1	3.1	2.9	3.1	2.8
T416 Oγ1	H421 Nε2	—	2.8	2.7	—	2.9	—	2.5
N417 N	N417 Oδ1	2.7	—	—	—	—	—	—
N417 Oδ1	S419 O^{γ}	3.0	—	—	—	—	—	—
S419 O^{γ}	H421 Nε2	—	—	—	—	—	2.8	—
I422 O	N423 Nδ2	—	2.9	—	—	—	—	b

"5B3" is hu5B3.v3, and "v362" is MRCT10.v362. Abbreviation: PDB, Protein Data Bank.
[a] No H-bond.
[b] One of the atoms is not present in coordinates.

robust resistance to neutralizing antibodies that bind the $E2^{412–423}$ epitope.

Structural analyses of MRCT10.v362 and hu5B3.v3 complexed with the $E2^{412–423\text{-GSGK-biotin}}$ peptide reveal that a glycan shift to N415 in the N417S and N417T E2 likely inhibits antibody binding

To determine whether the glycan shift to N415 in N417S E2 would affect antibody binding, we determined the crystal structures of hu5B3.v3 and MRCT10.v362 Fab fragments complexed with the $E2^{412–423\text{-GSGK-biotin}}$ peptide. The peptide configurations conform moderately well to the β-hairpins seen previously in complexes with the antibodies HCV1[30] and AP33.[31] For instance, most of the H-bonds within any version of the peptide are shared among all available structures of the peptide (Table 3). The close kinship of antibodies MRCT10.v362 and AP33 makes all four versions of the peptide seen in complexes with them especially similar, with rmsd values of C^{α} atoms from residues Ile414–His421 less than 0.15 Å. The analogous calculation using the HCV1-bound peptide is 0.35 Å. There is a distinguishing feature of the peptide complexed with hu5B3.v3; the presence of a type IV hairpin turn for residues Thr416–Ser419, where all other peptide structures have the more common type I′ turn. This results in an rmsd for comparison to the MRCT10.v362 peptide of 0.81 Å. The positions of the three E2 hydrophobic side chains most intimately contacting the antibodies, Leu413, Trp420 and Ile422, cluster in two groups after superposing the peptides, with those from the complexes with antibody HCV1 segregated from all others, including those from hu5B3.v3. The distances between analogous atoms when compared this way, about 3 Å, is probably no more than one expects for an exposed β-hairpin loop.

An array of H-bonds and hydrophobic contacts form the interface between the E2 peptide and hu5B3.v3 complementarity-determining region (CDR) loops H1, H2, H3, L1 and L3 (Tables S3 and S5). Since CDR loop L2 is not part of this paratope, the amino acid changes Gln54 → His and Gly55 → Ala, which provided enhanced affinity probably exert this influence via effects on the neighboring CDRs H1 and L1. An H-bonding interaction between the Asn415 side chain and Tyr96 (light chain) and the orientation of the E2 peptide with respect to the antibody are inconsistent with binding in the presence of glycan attached to Asn415 (Fig. 3).

All three MRCT10.v362 heavy-chain CDRs and light-chain CDRs L1 and L3 contact the E2 peptide, but there is only one residue each from CDRs H1 and H3 that is within 4 Å, Tyr 33 and Tyr100, respectively (Fig. S3b and Tables S4 and S5). Light-chain residue Tyr30, introduced during affinity maturation, has a hydrophobic contact with the Leu413 side chain, which the original Asn30 in AP33 does not provide. Ser98 of CDR H3, changed

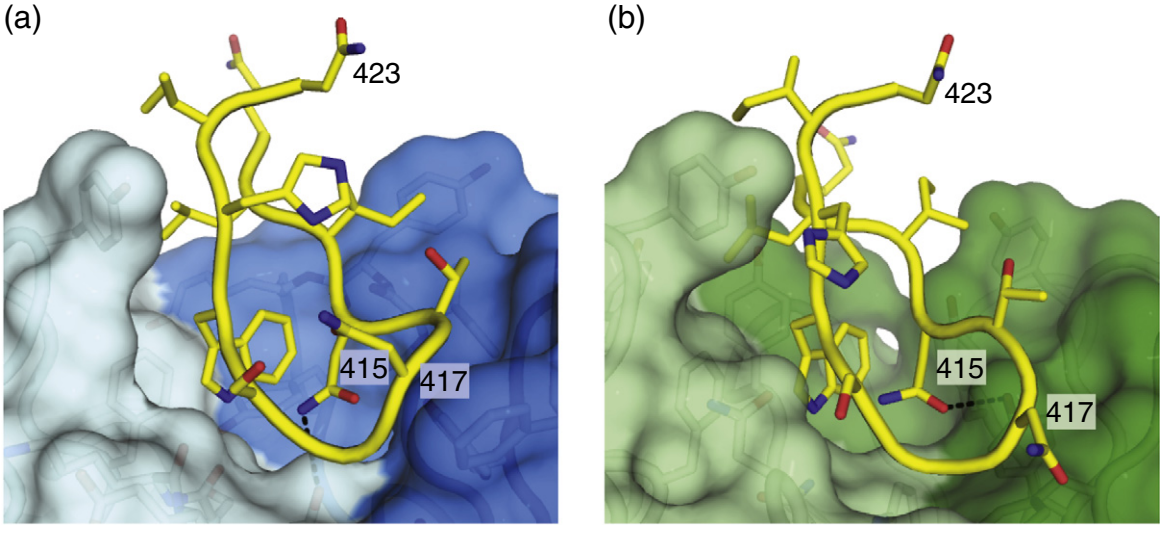

Fig. 3. Attachment of a glycan on E2 residue Asn415 would create an untenable steric clash with antibodies hu5B3.v3 and MRCT10.v362. (a) E2 peptide (yellow) directs the Asn415 side chain toward the Fab 5B3.v3 surface (light chain in light blue; heavy chain in dark blue), where it H-bonds with light-chain Tyr96 (broken line). (b) E2 peptide (yellow) directs the Asn415 side chain toward the Fab MRCT10.v362 surface (light chain in light green; heavy chain in dark green), where it H-bonds to heavy-chain Tyr50 (broken line). In both structures, the Asn415 side chain also stabilizes the peptide conformation via an H-bond with Gly418, as seen in prior work. Wild-type E2 sequences have glycan attached to residues Asn417 and Asn423. The side chains of these residues are directed away from the antibody, consistent with binding of 5B3 and MRCT10 when glycans are attached here.

from threonine during affinity maturation, does not contact the peptide so its role in binding $sE2_{661}$ protein is unclear. Similar to the finding for hu5B3.v3, an H-bond between the Asn415 side chain and MRCT10.v362 Tyr50 (heavy chain) and the peptide orientation with respect to the antibody preclude binding in the presence of a glycan attached at Asn415 (Fig. 3b).

The structural fidelity with which the humanized and affinity-matured MRCT10.v362 recapitulates the paratope of the original murine antibody AP33 is quite high. There are 13 antibody amino acid residues within 4.0 Å of the E2 peptide: light-chain residues Tyr28, Tyr30 (Asn30 in AP33), Phe32, Asn91, Asn92, Val93, Asp94 and Trp96 and heavy-chain residues Tyr33, Tyr50, Tyr53, Tyr58 and Tyr100. The rmsd for the superposition of 13 C^{α} pairs is only 0.15 Å. Comparison of C^{α} atoms for complete variable domains yields rmsd values of about 0.5 Å.

The two complexes in the crystallographic asymmetric unit of the MRCT10.v362/E2 peptide complex (referred to as ABZ and LHY according to protein chain identifiers for light chains, heavy chains and peptide, respectively) are similar overall, but a stark difference is seen between the two copies of CDR H1, which have quite different conformations for residues Gly26–Ser31 in CDR H1 (Figs. S4 and S5). The rmsd for superposition of the C^{α} atoms of these two segments is 1.9 Å. The CDR H1 from ABZ has intermolecular contacts less than 4 Å for residues Ser25, Gly26, Asp27 and Ser31, while there are none for CDR H1 from LHY. Thus, we find that CDR H1 from LHY adopts the very predominant canonical "H1-13-1" structure,[34] while that seen for ABZ seems to have been altered by the intermolecular contacts it experiences. Rather surprisingly, the conformation of CDR H1 found for AP33 alone and in complex with the E2 peptide is the unusual one ("H1-13-2"[34]), like that of ABZ, and this AP33 conformation arises without intermolecular contacts. The CDR H1 Tyr33 side chain hydroxyl H-bonds with the peptide, but Tyr33 is outside the part of this CDR that differs between the two copies. Thus, this conformational heterogeneity does not affect antigen recognition.

Combination of MRCT10 with other HCV antivirals results in enhanced suppression of infection and spread of resistant virus *in vitro*

In spite of the rapid emergence of the N417S-resistant mutant genotype 2a HCVcc *in vitro*, we suspected that combination of an entry inhibitor with an HCV DAA would enhance antiviral efficacy and perhaps suppress the emergence of resistant N417S HCVcc. Culturing of Huh7.5 cells in medium containing 1% dimethyl sulfoxide (DMSO) has been demonstrated to induce a non-dividing state and cause expression of hepatocyte-specific genes[35] and is an appropriate *in vitro* culture system to study HCV spread since there is no artificial viral spread arising from trypsinization. To determine if MRCT10.v362 could suppress the emergence of resistance to an approved HCV NS3 protease inhibitor (Telaprevir), we infected DMSO-differentiated Huh7.5 cells with Jc1 HCVcc alone or in the presence of Telaprevir, MRCT10.v362 or a combination of both Telaprevir and MRCT10.v362 (Fig. 4). A concentration of 2 μM Telaprevir was used, which is similar to the trough concentrations detected in some treated patients.[36] Jc1 HCVcc infection of DMSO-differentiated cells in the presence of Telaprevir induced early viral suppression but resulted in the emergence of a T54A HCVcc variant ~18 days post infection (Fig. 4). The T54A mutation has been demonstrated to confer resistance to Telaprevir and can be detected in some patients treated with Telaprevir monotherapy.[36,37] Treatment of cells with 10 μg/mL MRCT10.v362 resulted in no significant antiviral effect 10 days post infection, consistent with the rapid emergence of the MRCT10.v362-resistant variants, as detected previously. In comparison, combination of 10 μg/mL MRCT10.v362 with Telaprevir resulted in undetectable HCV RNA replication even at 22 days post infection when the T54A mutant emerged as the dominant resistant species in the Telaprevir-treated cultures.

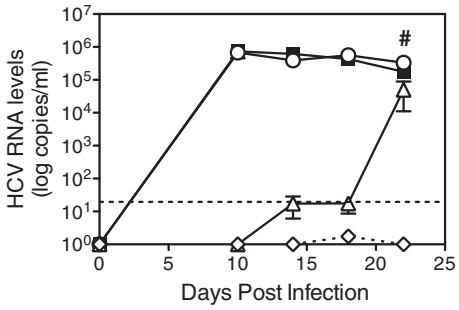

Fig. 4. Enhancement of antiviral effect of NS3 protease inhibitors by inhibition of HCV entry. DMSO-differentiated Huh7.5 cells were infected with Jc1 HCVcc (MOI = 0.05) alone (filled squares) or in the presence of MRCT10.v362 (10 μg/mL, open circles), Telaprevir (2 μM, open triangles) or a combination of MRCT10.v362 and Telaprevir (open diamonds). HCV RNA copies were measured at various times post infection as discussed in Materials and Methods. HCV cDNA derived from the day 22 post infection cultures was sequenced (denoted by the asterisk). These are representative data from two independent experiments.

Discussion

We have generated two independent affinity-matured neutralizing antibodies, hu5B3.v3 and

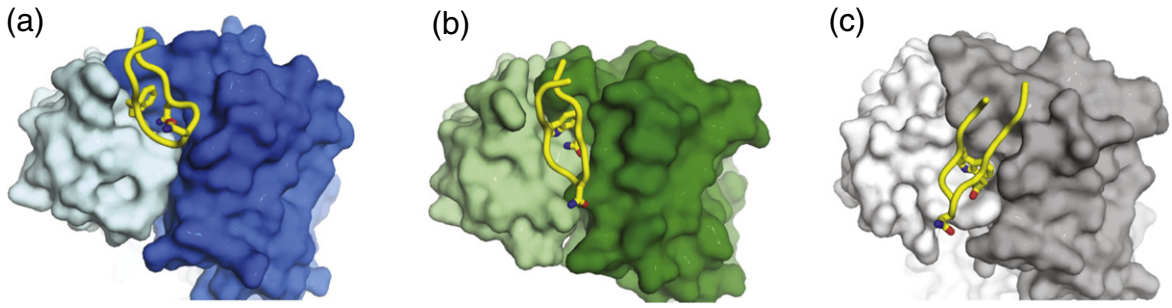

Fig. 5. The broadly neutralizing anti-HCV antibodies (a) hu5B3.v3 (light chain in light blue; heavy chain in dark blue), (b) MRCT10.v362 (light chain in light green; heavy chain in dark green) and (c) HCV1 (light chain in light gray; heavy chain in dark gray) recognize the same surface of the $E2^{412–423}$ epitope, but each with different details. After superpositioning using V_H domains, the Fab surfaces are shown with simplified peptide representation (yellow). Peptide side chains for Asn417, a glycan attachment point in wild-type sequences, and Trp420, central to the epitope, are shown as sticks.

MRCT10.v362, that bind to the $E2^{412–423}$ epitope and result in significant inhibition of HCVcc entry and infection *in vitro*. Using *in vitro* resistance selections, we have identified the N417S Jc1 HCVcc variant to be robustly resistant to all tested neutralizing antibodies that bind the $E2^{412–423}$ epitope, including the HCV1 antibody that is undergoing clinical testing in humans. Analysis of the glycosylation status of N415, N417 and N423 has revealed a glycosylation shift from residue 417 to N415 in the N417S and N417T mutant E2 glycoproteins, which plays an important role in the generation of resistance to broadly neutralizing antibodies. While recent work has shown that amino acid changes at residue N415 abrogate binding of another $E2^{412–423}$-specific neutralizing antibody (HCV1),[30] our studies show that changes in adjacent residues can shift glycan moieties to N415 and thereby produce an analogous escape from broadly neutralizing HCV antibodies.

Recent studies have proposed a structural basis for resistance to two broadly neutralizing antibodies, HCV1[30] and AP33.[29,31] Our structural results from both an independent neutralizing antibody and a humanized higher-affinity variant of AP33 are consistent with their findings. Together, these results suggest that most, if not all, HCV $E2^{412–423}$-specific neutralizing antibodies bind to a similar conformation of the $E2^{412–423}$ epitope, a β-hairpin with the glycosylated asparagines (N417 and N423) pointing away from the antibody surface. Nonetheless, each of the three antibodies, MRCT10.v362, hu5B3.v3 and HCV1, bind $E2^{412–423}$ using distinctly different antigen recognition surfaces (paratopes), as is made clear by ~7 Å distances between analogous peptide C^{α} atoms when the three structures are superposed using the V_H domains (Fig. 5). In addition, we find that W420, which has previously been found to be an essential contact site for binding CD81,[38] is buried in the peptide–antibody interface. Our alanine mutagenesis studies also revealed that W420 (and L413) are required for binding of both hu5B3.v3 and MRCT10.v362, consistent with what was recently shown for HCV1 and AP33.[29–31] Since W420 and N415 are in close proximity and on the same face of all $E2^{412–423}$ peptide structures reported to date, this raises a conceptual conflict regarding functions assigned to W420 (involved in CD81 binding) and glycosylated N415 (involved in preventing antibody binding). Nonetheless, as glycosylation of N415 does not seem to affect CD81 binding since HCV entry occurs in the N417S mutant, we are left to speculate that either the CD81–W420 interaction is relatively indirect or the β-hairpin is not the form of the $E2^{412–423}$ peptide during CD81 binding.

Interestingly, while binding of MRCT10.v362 was only modestly affected by the N415A mutation (3-fold decreased binding), it completely abrogated binding by hu5B3.v3 (Fig. 2a). While this effect on hu5B3.v3 is consistent with the presence in the hu5B3.v3/$E2^{412–423}$ complex of an H-bond between the Asn415 side chain and Tyr96 from the light chain, the MRCT10.v362/$E2^{412–423}$ complex includes an analogous H-bond between Asn415 and Tyr50 from the heavy chain (Fig. S3). Similarly, there is a big discrepancy in the effects on antibody affinity for the G418A mutant peptide—even though the peptide backbone conformation for Gly418 from the crystal structures is one that is relatively intolerant of any other amino acid, the measured effects of Alanine substitution are ~2-fold (MRCT10.v362) and ~200-fold (hu5B3.v3). In contrast, while the HCV1 antibody does not bind the N415A peptide, there is no H-bonding between N415 and HCV1.[30] These data show that the useful concept of a widely conserved epitope recognized by neutralizing antibodies does not extend to close similarities in residue-specific contributions of that epitope to binding energies. Thus, while L413 and W420 are generally required for tight binding by $E2^{412–423}$-specific neutralizing antibodies, different antibodies may utilize different additional residues. How this impacts the breadth of neutralization by $E2^{412–423}$-

specific antibodies and the number of mutations that could lead to escape is an intriguing question and will require additional studies.

Glycosylation at N415 in the N417S HCVcc plays an important role in mediating resistance to hu5B3.v3 and MRCT10.v362 as there was a cumulative 82-fold increase in N417S and N417T mutations as early as 5 days post treatment with AP33 identified by ultra deep sequencing. This is particularly interesting since both N417S and N417T mutations result in a shift of the glycan from residue 417 to N415, suggesting that the presence of a glycan at N415 is preferred during early antibody pressure. Based on our structural results, it is straightforward to predict that the glycan shift to N415 will result in resistance to hu5B3.v3 and MRCT10.v362 and probably most if not all other $E2^{412–423}$-specific neutralizing antibodies. While the N417 side chain is pointing away from both hu5B3.v3 and MRCT10.v362 Fab faces, the N415 side chain is buried in the peptide–antibody interface and involved in H-bonds with antibody side chains. The presence of even a single glycan residue at this position is quite inconsistent with all the interactions seen between peptide and the Fabs—there is simply no room. N417 is a bona fide N-linked glycosylation site and HCVpp containing an N417Q mutation in E2, which results in the loss of glycosylation at that site, was demonstrated to be ~50% more sensitive to neutralization by AP33 compared to the wild-type HCVpp. This led the authors to propose that the N417 glycan may be masking the $E2^{412–423}$ epitope from broadly neutralizing antibodies.[26,39] Our data suggest that this may not apply to all $E2^{412–423}$-specific neutralizing antibodies since the N417G Jc1 HCVcc mutant, which like the N417Q virus is not glycosylated at either residue 415 or residue 417, is no more sensitive to neutralization by AP33 and MRCT10.v362. In fact, N417G Jc1 HCVcc is 11-fold and 18-fold more resistant to two other $E2^{412–423}$-specific antibodies, hu5B3.v3 and HCV1, respectively (Table 2). These data suggest that, at least in genotype 2a HCV, the N417 glycan may not be as important for evasion against $E2^{412–423}$-specific antibodies and that specific mutations at N417 may play different roles in determining the affect on neutralization by $E2^{412–423}$-specific antibodies.

The role of glycosylation in regulating resistance to neutralizing antibodies has been extensively studied for human immunodeficiency virus 1.[40–44] In particular, human immunodeficiency virus 1 escape from neutralizing antibodies also involves changes in N-linked glycosylation that conferred escape from autologous patient antibodies and epitope-specific monoclonal antibodies.[40] Our data suggest that multiple viruses, including HCV, may have evolved mechanisms to shift their glycan shield in order to escape from potent neutralizing antibodies. While the N417S-resistant virus can be detected in genotype 1 HCV-infected chimpanzees[45] and HCV isolates containing mutations at N415 and N417 were also detected in HCV-infected patients undergoing liver transplants who were administered the HCV1 antibody,[46] we are encouraged to learn that, in spite of the robust *in vitro* resistance of the N417S mutant virus to $E2^{412–423}$-specific neutralizing antibodies, the combination with other HCV antivirals not only resulted in synergistic antiviral efficacy but also suppressed the emergence of resistance to both the HCV protease inhibitor Telaprevir and MRCT10.v362. These data demonstrate that entry inhibition may also serve as a novel salvage antiviral mechanism in patients who do not respond well to other HCV DAAs and inform the development of novel HCV vaccine antigens that would allow for the development of a broadly reactive neutralizing antibody response.

Materials and Methods

Development and characterization of mouse anti-HCV E2 antibody 5B3 (mu5B3)

Balb/c mice (Charles River, Hollister, CA) were primed with 10 μg pORF-mFlt3L plasmid DNA, followed with weekly immunizations of 50 μg plasmid DNA encoding HCV E1–E2 and 2.5 μg mGM-CSF plasmid DNA (Genentech) diluted in lactated Ringer's solution via hydrodynamic tail vein injection as previously described.[47–49] Serum was screened for neutralizing activity against genotypes 1a and 1b HCVpp. Three days following the last hydrodynamic tail vein immunization, splenocytes were taken from the mouse that showed strongest neutralization activity and fused with X63-Ag8.653 mouse myeloma cells (American Type Culture Collection, Rockville, MD) via electrofusion (Cytopulse, Glen Burnie, MD), then incubated at 37 °C, 7% CO_2, overnight in Dulbecco's modified Eagle's medium (DMEM; Lonza, Basel, Switzerland) supplemented with 10% fetal bovine serum, 4.5 g/L glucose, 25 mM Hepes, 0.15 mg/mL oxaloacetic acid, 100 μg/mL pyruvic acid, 0.2 U/mL insulin, 2 mM L-glutamine, 100 U/mL penicillin and 100 μg/mL streptomycin (Invitrogen, Carlsbad, CA), NCTC-109 (Lonza, Allendale, NJ) and NEAA (Invitrogen), before plating into 96-well plates supplemented with 5.7 μM azaserine and 100 μM hypoxanthine (Sigma-Aldrich, St. Louis, MO). Supernatants were screened for IgG production by ELISA 11 days post-fusion and tested for binding to 293 cells transiently transfected with HCV E1E2-expressing plasmids by fluorescence-activated cell sorter. Hybridomas demonstrating strong HCV glycoprotein-specific binding by fluorescence-activated cell sorter were screened for neutralizing activity against GT1a, GT1b and GT2a HCVpp. One neutralizing antibody clone, 5B3, was expanded and subcloned by two rounds of limiting dilution, then expanded for large-scale production in bioreactors (Integra Biosciences, Chur, Switzerland). Supernatant was then purified by protein A affinity chromatography as previously described.[49]

Antibody binding measurements

The HCV amino acid positions are numbered according to the genotype 1a H77 polyprotein sequence. Sequence changes resulting in apparent improved affinity were transferred into mammalian IgG expression vectors, transiently expressed in CHO (*C*hinese *h*amster *o*vary) cells and purified by affinity chromatography on protein A Sepharose. SPR measurements of $sE2_{661}$ binding to antibody were performed on a Biacore 4000 instrument (GE Healthcare, Pittsburgh, PA) using the human antibody capture kit as described by the manufacturer. Sensorgrams were recorded for injections of 60 µL at 30 µL/min of solutions of $sE2_{661}$ ranging in concentration from 1.5 nM to 100 nM in 2-fold increments. Kinetic constants were determined using 4000 Evaluation Software v1.0. Fab fragments were prepared by LysC endoprotease cleavage of intact IgG as previously demonstrated.[50] Dissociation constants (K_D) for Fab binding to peptide epitope QLINTNGSWHIN attached to biotin via a GSGK linker ($E2^{412–423\text{-}GSGK\text{-}biotin}$) were determined by bio-layer interferometry on a ForteBio Octet Red384. Briefly, streptavidin biosensor tips were incubated with 5 µg/mL biotinylated peptide followed by 100 nM Fab. Binding constants were calculated from the response profile using Data Analysis Software v6.4.

To detect antibody binding to HCV E1E2-expressing 293T cells by ELISA, we coated 96-well Immulon™ 2 HB plates (Immunochemistry Technologies, Bloomington, MN) with 0.25 µg/well GNA (*Galanthus nivalis l*ectin) overnight at room temperature. Plates were washed 6× with phosphate-buffered saline (PBS) containing 0.02% Tween 20. GNA-coated plates were then incubated with lysates of 293T cells transfected with plasmids encoding HCV E1–E2 from genotypes 1a (H77), 1b (Con1) and 2a (J6) for 2 h at room temperature. Plates were washed 6× with PBS containing 0.02% Tween 20 followed by incubation with 5 mg/mL of AP33, MRCT10.v362, mu5B3, hu5B3.v3 and HCV1 antibodies for 2 h at room temperature. Binding was detected using anti-human and anti-mouse horseradish-peroxidase-conjugated antibodies and TMB substrate (Rockland Immunochemicals, Gilbertsville, PA). The reaction was stopped by adding 1 M phosphoric acid and an OD_{450} was measured using a Synergy 2 Microplate Reader (Biotek, Winooski, VT).

Tissue culture and generation of full-length infectious HCVcc cDNA

Huh7.5 cells were obtained from Apath LLC under license and cultured in complete DMEM (supplemented with 10% fetal calf serum, 100 U/mL penicillin, 100 mg/mL streptomycin, 2 mM L-glutamine and 0.1 mM non-essential amino acids).[51–53] The J6/C3 (Jc1; genotype 2a) and bicistronic Con1/C3 (genotype 1b) chimeric genomes were generated as previously described.[54]

Generation of infectious HCVcc and HCVpp stocks

Jc1 and Con1/C3-neo HCVcc virus stocks were generated by transfecting Huh7.5 cells with *in vitro* transcribed full-length HCV RNA as described previously.[53,54] Plasmids were linearized with XbaI and *in vitro* transcribed RNA was generated using Megascript Kit (Life Technologies, Grand Island, NY) as per manufacturer's instructions. HCV RNA was transfected into Huh7.5 cells by electroporation as described previously.[53,54] Supernatants from Jc1 RNA-transfected cells were harvested starting from 3 days post transfection, titered and pooled to generate laboratory stocks. HCVcc titers were measured using the $TCID_{50}$ calculator as described previously.[55] HCVpp stocks were generated as previously described.[54]

Antibodies used in HCV neutralization assays

Genes for the HCV1 antibody heavy- and light-chain variable domains were synthesized (Blue Heron Inc., Bothell, WA) on the basis of the published amino acid sequence (Ref. 17; patent application PCT/US2008/001922). Sequences were codon optimized for expression in mammalian cells. The variable heavy domain was cloned on an EcoRI/ApaI fragment into a human IgG1 expression plasmid.[56] Similarly, the variable light domain was cloned on an EcoRI/BlpI fragment into a human kappa light-chain expression plasmid. HCV1 protein was transiently produced by co-transfection of CHO cells with an equimolar mixture of heavy- and light-chain expression plasmids and antibody was purified by affinity chromatography on protein A Sepharose. Anti-CD81 clone JS-81 (BD Pharmingen, San Diego, CA) and anti-CLDN1 clone 5.16v5[54] were used as controls for HCV neutralization assays.

Neutralization assays

Multiplicity of infection (MOI) for Jc1 HCVcc was calculated based on virus titer as measured by $TCID_{50}$ calculations.[55] HCVpp stocks were normalized for luciferase activity before infecting cells. Neutralization assays using HCVpp or HCVcc viruses were performed as described previously.[54,57]

RNA extractions, reverse transcription and real-time quantitative PCR analysis

Real-time quantitative PCR analysis was performed as described previously.[51,54,57] Data were analyzed using relative expression ($2^{-\Delta\Delta CT}$ method) normalized to GAPDH as described previously.[52,58]

Ultra deep sequencing of *in vitro* resistance selection and chronic patient sera

Total RNA was extracted from $\sim 5 \times 10^4$ cells per sample (per 24 wells) using RNeasy Mini spin columns. HCV E1E2 cDNA was generated using One-Step RT-PCR kit (Qiagen) according to the manufacturer's instructions using the following primers: (sense) 5′-GGAGGACGGGGTTAATTTTG-3′ and (antisense) 5′-CCCGACCCTTGATGTACCAA-3′. The E1E2 cDNAs were used as templates to generate ~200-bp PCR products covering the $E2^{412–423}$ epitope using primers tagged with 454 barcodes as listed in Table S1. All PCR products were gel-purified before 454 sequencing (454 Life Sciences, Branford, CT).

Roche 454 sequencing data were analyzed using in-house computer programs. Briefly, a data-processing pipeline was established to handle sequence read files and the quality score files simultaneously and to detect barcode errors. Reads were binned using 5′ and 3′ barcodes and translated in the appropriate frame. Sequence reads with <100 nucleotides were filtered out, together with translated sequences that did not contain a predefined amino acid motif adjacent to the region of interest. The pipeline was used to generate amino acid frequencies for code pairs, consensus sequences and amino acid frequencies at specific positions for each code pair.

Protein purification and mass spectrometric analysis

We seeded 5×10^6 Huh7.5 cells in T225 flasks, and the following day, we transfected the cells with a plasmid expressing soluble genotype 2a J6CF $sE2_{661}$ containing either wild-type (N417) or mutant residues (N417G, N417S, N417T) using Lipofectamine 2000, according to the manufacturer's instructions. After incubation with the Lipofectamine–DNA mix for 5 h, media was replaced with DMEM supplemented with fetal bovine serum (2% final concentration). After 72 h, supernatant was collected and clarified using a 0.2 μM filter. Fifty milliliters of the transfected Huh7.5 conditioned media was batched at 4 °C with Ni-NTA resin and then processed in column format. The column was washed with PBS, 1 mM azide (Buffer A) down to baseline, followed by 25 mM imidazole with 0.3 M sodium chloride in Buffer A to baseline then eluted with 250 mM imidazole and 0.3 M sodium chloride in Buffer A. Five micrograms of the eluted protein was reduced with 10 mM dithiothreitol and alkylated with 15 mM *N*-isopropyl-2-iodoacetamide. The alkylation reaction was stopped with 250 mM β-mercaptoethanol, and the sample was added to SDS sample buffer, separated on a SDS gel then transblotted to a polyvinylidene fluoride membrane.

HCV electroblotted sample bands were excised, blocked with 0.5% Zwittergent 3–16 (Calbiochem, Billerica, MA) and deglycosylated with PNGase F (New England Biolabs) in 50 mM Tris–HCl (pH 8.0) for 2 h at 45 °C. The deglycosylated samples were then digested with 0.2 μg trypsin (Promega, Madison, WI) in 10% acetonitrile/100 mM Tris (pH 8.0) for 1 h at 37 °C. Equivalent samples treated with non-PNGase F were processed in parallel. The digested samples were analyzed by capillary reverse phase ultra-performance liquid chromatography (UPLC) electrospray ionization MS/MS on an LTQ-Orbitrap XL mass spectrometer (ThermoElectron, Madison, WI). Samples were loaded in 0.1% trifluoroacetic acid in water onto a 100-μm i.d. capillary column (nanoAcquity UPLC column, 100 μm × 100 nm, 1.7 μm, BEH130 C18; Waters Corp). Peptides were eluted with a 45-min gradient of 5–90% Buffer B (where Buffer A was composed of 0.1% formic acid in water and Buffer B was composed of 0.1% formic acid in acetonitrile) at 1.00 μL/min generated by a UPLC system (nanoAcquity UPLC; Waters Corp). Mass spectral data were acquired using methods that included one full MS scan (400–1600 *m*/*z*) in the Orbitrap at resolution of 60,000 M/ΔM at *m*/*z* 400 followed by collision-induced dissociation of the top 5 most abundant ions detected in the full MS scan and several targeted product ion scans in the ion trap. Ions chosen for targeted experiments included the doubly charged HCV tryptic peptides containing N415, N417 and N423 in their potential non-deamidated and deamidated states. The tandem mass spectral results were submitted for database searching using the Mascot program (Matrix Science) against an in-house curated protein database and the Swiss-Prot database. The following search parameters were specified: full trypticity, one miscleavage, variable modifications on Asn/Gln deamidation (+0.984 Da), Met oxidation (+15.995 Da), Cys *N*-isopropyl carboxamidomethylation (+99.068 Da), 20 ppm precursor ion mass and 0.5 Da fragment ion mass tolerance. Deamidated peptide identifications were confirmed by manual interpretation of mass spectral data.

Antibody/antigen complex preparation

Fab fragments of hu5B3.v3 and MRCT10.v362 were diluted using 0.6% acetic acid and each was loaded onto a 5-mL *S*-Sepharose fast flow cation-exchange column and eluted with a 10 CV linear gradient from 25 mM 4-morpholineethanesulfonic acid (Mes) (pH 5.5) to 0.5 M NaCl and 25 mM Mes (pH 5.5). The peak fractions were pooled and concentrated to 20 mg/mL. A 2-fold molar excess of $E2^{412–423\text{-GSGK-biotin}}$ was added to each of the Fab fragments and incubated for 12 h at 4 °C. The protein complexes were screened for crystallization in sitting drops using the Phoenix robot (Art Robbins) and commercial screening solutions. Crystallization droplets consisted of 0.2 μL protein and 0.2 μL reservoir at 18 and 4 °C. The 5B3.v3/E2 complex crystallized after 2 days with 0.1 M Mes (pH 6.0) and 2.4 M ammonium sulfate at 18 °C. A cryoprotectant consisting of glycerol 25% (v/v) final concentration added to the reservoir permitted preservation by immersion in liquid nitrogen. The MRCT10.v362/E2 complex crystallized after several months in 0.1 M LiCl, 20% (w/v) polyethylene glycol 6000 and 0.1 M Tris (pH 8.5) at 18 °C. Polyethylene glycol 3350 25% (w/v) final was added to the reservoir and harvested crystals were preserved by immersion in liquid nitrogen.

Hu5B3.v3 Fab/$E2^{412–423\text{-GSGK-biotin}}$ structure determination

Data in a tetragonal point group extending to 2.6 Å resolution were collected at Stanford Synchrotron Radiation Lightsource beamline 11–1. Data reduction (HKL2000[59]) and structure solution by molecular replacement (Phaser[60]) allowed assignment of the space group as $P4_12_12$. The molecular replacement search probes were separate constant region and Fv fragments searched stepwise, and the Fv fragment lacked CDR loop regions. After care was taken to identify CDR loops in the initial electron density maps, a tentative polyalanine peptide was built (Coot[61]). After refinement of this model, electron density suggestive of the peptide side chains permitted confident assignment of the peptide direction and sequence. Refinement was performed using Phenix[62] and Refmac5[63] and included TLS treatment of thermal factors. The E2-derived peptide is resolved from Gln412 to Asn423, leaving the linker residues 424–427 (Gly-Ser-Gly-Lys) and the C-terminal biotin unresolved. A flat $F_o - F_c$ map in the E2 peptide region was obtained using main-

Table 4. Data collection and refinement for Fab/E2$^{412–423\text{-GSGK-biotin}}$ complexes

	FabMRCT10.v362/pep	Fab5B3.v3/pep
Data collection	CLS 08ID-1	SSRL 11-1
Space group	$P2_1$	$P4_12_12$
Unit cell parameters		
a, *b*, *c* (Å)	71.09, 90.82, 72.68	77.72, 77.72, 181.4
α, *β*, *γ* (°)	90, 109.3, 90	90, 90, 90
V_M (Å^3/Da)	2.3	2.9
Resolution (Å)	50–1.53	50–2.60
R_{sym}[a,b]	0.052 (0.552)	0.098 (0.713)
Number of observations	487,066	137,676
Unique reflections	131,070	17,880
Completeness (%)[b]	99.9 (99.2)	99.9 (100)
$I/\sigma I$[b]	23.0 (2.2)	19.2 (3.2)
Wilson *B* (Å^2)	21	72
Refinement		
Resolution (Å)	50–1.53	50–2.60
Refs. [$F > 0(\sigma F)$]	129,605	17,838
Final R_{cryst},[c] R_{free}	0.175, 0.200	0.222, 0.264
Molecules per asymmetric unit	2	1
Protein residues	889	455
Solvent molecules	1059	36
Atoms	7968	3540
Non-crystallographic symmetry rmsd (light chain, heavy chain, peptide) (Å)	0.73, 0.81, 0.49	Not applicable
Mean *B*-factor (light chain/heavy chain/peptide/water/all) (Å^2)	25/21/26/28/24 25/22/27/—/—	62/67/78/53/65
rmsd bonds (Å)	0.008	0.009
rmsd angles (°)	1.2	1.3
Number of TLS groups	23	5
Ramachandran (%)	96/3/1	95/4/1

[a] $R_{sym} = \sum|I - \langle I\rangle|/\sum\langle I\rangle$, where I is the intensity of a single observation and $\langle I\rangle$ is the average intensity for symmetry-equivalent observations.
[b] Values in parentheses are for the highest-resolution shell.
[c] $R_{cryst} = \sum|F_o - F_c|/\sum|F_o|$, where F_o and F_c are observed and calculated structure factor amplitudes, respectively. R_{free} is calculated as R for reflections sequestered from refinement.

chain torsion angles for residues 417 and 418 best described as type IV turn, which produces a close contact for H-atoms on the adjacent amide nitrogen atoms of T416 and N417. Reference to the higher-resolution MRCT0.v362/ E2$^{412–427\text{-GSGK-biotin}}$ structure permitted a refinement experiment that relieved this apparent clash but that resulted in relatively large $F_o - F_c$ features, which could be accounted for by the original model that was therefore retained (Fig. S6). Data reduction and final refinement statistics appear in Table 4.

MRCT10.v362 Fab/E2$^{412–423\text{-GSGK-biotin}}$ structure determination

Data in the monoclinic point group extending to 1.53 Å resolution were collected at Canadian Light Source beamline 08ID-1 by Shamrock Structures, LLC (Woodridge, IL). Data reduction and structure solution (in space group $P2_1$) were performed as above, except that the asymmetric unit contains two complexes. After building all CDR loops, extra electron density was assigned to the E2 peptide. Optimal fit of the peptide from the Fab5B3 complex required adjustment of the peptide residues 415–417. Non-crystallographic symmetry restraints were applied between all three pairs of homologous polypeptides, and TLS treatment of thermal factors was used. Data reduction and final refinement statistics appear in Table 4.

Jc1 HCVcc infection of DMSO-differentiated Huh7.5 cells

Huh7.5 cells (90% confluent) were cultured in collagen-coated, 96-well plates in the presence of complete DMEM containing 1% DMSO. Culture media was replenished every 2 days for 14 days after which cells were infected with Jc1 HCVcc (MOI = 0.05). One day post infection, cells were treated with either 10 μg/mL MRCT10-v362 or 2 μM Telaprevir alone or in combination. Fresh inhibitors were added every 2 days until day 22 post infection. HCV RNA replication was measured at various times post infection by real-time quantitative PCR as described above.

Statistical analyses

All statistical analyses were performed using GraphPad Prism software (GraphPad, San Diego, CA). All graphs represent the mean ± standard error of the mean (SEM) unless stated otherwise. *p* values for all data were determined using the regular *t* test unless otherwise

indicated (p values: *$p < 0.05$, **$p < 0.01$ and ***$p < 0.001$ are denoted when appropriate).

Accession numbers

Final coordinates and structure factors from MRCT10.v362 and hu5B3.v3 Fabs complexed with E2 peptide have been deposited in the Protein Data Bank under accession codes 4HS6 and 4HS8, respectively.

Acknowledgements

The authors thank Sophia Lee for preparation of Fab fragments. D.J.M., A.B. and A.H.P. generated MRCT10; H.P., J.D., M.U., M.H., M.M., K.M., K.T., T.K.C. and R.F.K. performed all remaining experiments; S.B.K., R.F.K. and C.E. reviewed the data and wrote the manuscript, and S.B.K. designed the overall experimental strategy. All authors except D.J.M., A.B. and A.H.P. are employees of Genentech (a member of the Roche Group) and shareholders of Roche. This study was supported by internal Genentech funds. Diffraction data were collected at the Stanford Synchrotron Radiation Lightsource, operated for the U.S. Department of Energy Office of Science by Stanford University and supported by the Department of Energy Office of Biological and Environmental Research, National Institutes of Health, National Institute of General Medical Sciences (including P41GM103393) and the National Center for Research Resources (P41RR001209), and at the Canadian Light Source, which is supported by the Natural Sciences and Engineering Research Council of Canada, the National Research Council Canada, the Canadian Institutes of Health Research, the Province of Saskatchewan, Western Economic Diversification Canada and the University of Saskatchewan. The work that led to the generation of MRCT10 (D.J.M., A.B. and A.H.P.) was supported by the Medical Research Council, United Kingdom.

Supplementary Data

Supplementary data to this article can be found online at http://dx.doi.org/10.1016/j.jmb.2013.02.025

Received 30 October 2012;
Received in revised form 15 February 2013;
Accepted 22 February 2013
Available online 28 February 2013

Keywords:
glycan shielding;
neutralizing antibody escape;
virus;
β-hairpin epitope

† H.P. and J.D. contributed equally to this work.

Abbreviations used:
HCV, hepatitis C virus; UTR, untranslated region; DAA, direct acting antiviral; SPR, surface plasmon resonance; CDR, complementarity-determining region; DMSO, dimethyl sulfoxide; DMEM, Dulbecco's modified Eagle's medium; PBS, phosphate-buffered saline; MOI, multiplicity of infection; UPLC, ultra-performance liquid chromatography; MS, mass spectrometry; Mes, 4-morpholineethanesulfonic acid; SEM, standard error of the mean.

References

1. Bradley, D. W. (2000). Studies of non-A, non-B hepatitis and characterization of the hepatitis C virus in chimpanzees. *Curr. Top. Microbiol. Immunol.* **242**, 1–23.
2. Trowbridge, R. & Gowans, E. J. (1998). Identification of novel sequences at the 5′ terminus of the hepatitis C virus genome. *J. Viral Hepat.* **5**, 95–98.
3. Blight, K. J. & Rice, C. M. (1997). Secondary structure determination of the conserved 98-base sequence at the 3′ terminus of hepatitis C virus genome RNA. *J. Virol.* **71**, 7345–7352.
4. McCaffrey, A. P., Ohashi, K., Meuse, L., Shen, S., Lancaster, A. M., Lukavsky, P. J. *et al.* (2002). Determinants of hepatitis C translational initiation *in vitro*, in cultured cells and mice. *Mol. Ther.* **5**, 676–684.
5. Tsukiyama-Kohara, K., Iizuka, N., Kohara, M. & Nomoto, A. (1992). Internal ribosome entry site within hepatitis C virus RNA. *J. Virol.* **66**, 1476–1483.
6. Wang, C., Sarnow, P. & Siddiqui, A. (1993). Translation of human hepatitis C virus RNA in cultured cells is mediated by an internal ribosome-binding mechanism. *J. Virol.* **67**, 3338–3344.
7. Friebe, P. & Bartenschlager, R. (2002). Genetic analysis of sequences in the 3′ nontranslated region of hepatitis C virus that are important for RNA replication. *J. Virol.* **76**, 5326–5338.
8. Yi, M. & Lemon, S. M. (2003). 3′ nontranslated RNA signals required for replication of hepatitis C virus RNA. *J. Virol.* **77**, 3557–3568.
9. Yi, M. & Lemon, S. M. (2003). Structure–function analysis of the 3′ stem-loop of hepatitis C virus genomic RNA and its role in viral RNA replication. *RNA*, **9**, 331–345.
10. Bartenschlager, R. & Lohmann, V. (2000). Replication of hepatitis C virus. *J. Gen. Virol.* **81**, 1631–1648.
11. Reed, K. E. & Rice, C. M. (2000). Overview of hepatitis C virus genome structure, polyprotein processing, and protein properties. *Curr. Top. Microbiol. Immunol.* **242**, 55–84.
12. Pileri, P., Uematsu, Y., Campagnoli, S., Galli, G., Falugi, F., Petracca, R. *et al.* (1998). Binding of hepatitis C virus to CD81. *Science*, **282**, 938–941.
13. Scarselli, E., Ansuini, H., Cerino, R., Roccasecca, R. M., Acali, S., Filocamo, G. *et al.* (2002). The human scavenger receptor class B type I is a novel candidate receptor for the hepatitis C virus. *EMBO J.* **21**, 5017–5025.

14. Benedicto, I., Molina-Jimenez, F., Bartosch, B., Cosset, F. L., Lavillette, D., Prieto, J. *et al.* (2009). The tight junction-associated protein occludin is required for a postbinding step in hepatitis C virus entry and infection. *J. Virol.* **83**, 8012–8020.
15. Ploss, A., Evans, M. J., Gaysinskaya, V. A., Panis, M., You, H., de Jong, Y. P. & Rice, C. M. (2009). Human occludin is a hepatitis C virus entry factor required for infection of mouse cells. *Nature*, **457**, 882–886.
16. Evans, M. J., von Hahn, T., Tscherne, D. M., Syder, A. J., Panis, M., Wolk, B. *et al.* (2007). Claudin-1 is a hepatitis C virus co-receptor required for a late step in entry. *Nature*, **446**, 801–805.
17. Broering, T. J., Garrity, K. A., Boatright, N. K., Sloan, S. E., Sandor, F., Thomas, W. D., Jr. *et al.* (2009). Identification and characterization of broadly neutralizing human monoclonal antibodies directed against the E2 envelope glycoprotein of hepatitis C virus. *J. Virol.* **83**, 12473–12482.
18. Flint, M., Maidens, C., Loomis-Price, L. D., Shotton, C., Dubuisson, J., Monk, P. *et al.* (1999). Characterization of hepatitis C virus E2 glycoprotein interaction with a putative cellular receptor, CD81. *J. Virol.* **73**, 6235–6244.
19. Owsianka, A., Clayton, R. F., Loomis-Price, L. D., McKeating, J. A. & Patel, A. H. (2001). Functional analysis of hepatitis C virus E2 glycoproteins and virus-like particles reveals structural dissimilarities between different forms of E2. *J. Gen. Virol.* **82**, 1877–1883.
20. Owsianka, A., Tarr, A. W., Juttla, V. S., Lavillette, D., Bartosch, B., Cosset, F. L. *et al.* (2005). Monoclonal antibody AP33 defines a broadly neutralizing epitope on the hepatitis C virus E2 envelope glycoprotein. *J. Virol.* **79**, 11095–11104.
21. Perotti, M., Mancini, N., Diotti, R. A., Tarr, A. W., Ball, J. K., Owsianka, A. *et al.* (2008). Identification of a broadly cross-reacting and neutralizing human monoclonal antibody directed against the hepatitis C virus E2 protein. *J. Virol.* **82**, 1047–1052.
22. Giang, E., Dorner, M., Prentoe, J. C., Dreux, M., Evans, M. J., Bukh, J. *et al.* (2012). Human broadly neutralizing antibodies to the envelope glycoprotein complex of hepatitis C virus. *Proc. Natl Acad. Sci. USA*, **109**, 6205–6210.
23. Goffard, A., Callens, N., Bartosch, B., Wychowski, C., Cosset, F. L., Montpellier, C. & Dubuisson, J. (2005). Role of N-linked glycans in the functions of hepatitis C virus envelope glycoproteins. *J. Virol.* **79**, 8400–8409.
24. Angus, A. G. & Patel, A. H. (2011). Immunotherapeutic potential of neutralizing antibodies targeting conserved regions of the HCV envelope glycoprotein E2. *Future Microbiol.* **6**, 279–294.
25. Falkowska, E., Kajumo, F., Garcia, E., Reinus, J. & Dragic, T. (2007). Hepatitis C virus envelope glycoprotein E2 glycans modulate entry, CD81 binding, and neutralization. *J. Virol.* **81**, 8072–8079.
26. Helle, F., Goffard, A., Morel, V., Duverlie, G., McKeating, J., Keck, Z. Y. *et al.* (2007). The neutralizing activity of anti-hepatitis C virus antibodies is modulated by specific glycans on the E2 envelope protein. *J. Virol.* **81**, 8101–8111.
27. Helle, F., Vieyres, G., Elkrief, L., Popescu, C. I., Wychowski, C., Descamps, V. *et al.* (2010). Role of N-linked glycans in the functions of hepatitis C virus envelope proteins incorporated into infectious virions. *J. Virol.* **84**, 11905–11915.
28. Dhillon, S., Witteveldt, J., Gatherer, D., Owsianka, A. M., Zeisel, M. B., Zahid, M. N. *et al.* (2010). Mutations within a conserved region of the hepatitis C virus E2 glycoprotein that influence virus-receptor interactions and sensitivity to neutralizing antibodies. *J. Virol.* **84**, 5494–5507.
29. Kong, L., Giang, E., Nieusma, T., Robbins, J. B., Deller, M. C., Stanfield, R. L. *et al.* (2012). Structure of hepatitis C virus envelope glycoprotein E2 antigenic site 412 to 423 in complex with antibody AP33. *J. Virol.* **86**, 13085–13088.
30. Kong, L., Giang, E., Robbins, J. B., Stanfield, R. L., Burton, D. R., Wilson, I. A. & Law, M. (2012). Structural basis of hepatitis C virus neutralization by broadly neutralizing antibody HCV1. *Proc. Natl Acad. Sci. USA*, **109**, 9499–9504.
31. Potter, J. A., Owsianka, A. M., Jeffery, N., Matthews, D. J., Keck, Z. Y., Lau, P. *et al.* (2012). Toward a hepatitis C virus vaccine: the structural basis of hepatitis C virus neutralization by AP33, a broadly neutralizing antibody. *J. Virol.* **86**, 12923–12932.
32. Gal-Tanamy, M., Keck, Z. Y., Yi, M., McKeating, J. A., Patel, A. H., Foung, S. K. & Lemon, S. M. (2008). *In vitro* selection of a neutralization-resistant hepatitis C virus escape mutant. *Proc. Natl Acad. Sci. USA*, **105**, 19450–19455.
33. Iacob, R. E., Perdivara, I., Przybylski, M. & Tomer, K. B. (2008). Mass spectrometric characterization of glycosylation of hepatitis C virus E2 envelope glycoprotein reveals extended microheterogeneity of N-glycans. *J. Am. Soc. Mass Spectrom.* **19**, 428–444.
34. North, B., Lehmann, A. & Dunbrack, R. L., Jr (2011). A new clustering of antibody CDR loop conformations. *J. Mol. Biol.* **406**, 228–256.
35. Sainz, B., Jr. & Chisari, F. V. (2006). Production of infectious hepatitis C virus by well-differentiated, growth-arrested human hepatoma-derived cells. *J. Virol.* **80**, 10253–10257.
36. Reesink, H. W., Zeuzem, S., Weegink, C. J., Forestier, N., van Vliet, A., van de Wetering de Rooij, J. *et al.* (2006). Rapid decline of viral RNA in hepatitis C patients treated with VX-950: a phase Ib, placebo-controlled, randomized study. *Gastroenterology*, **131**, 997–1002.
37. Sarrazin, C., Kieffer, T. L., Bartels, D., Hanzelka, B., Muh, U., Welker, M. *et al.* (2007). Dynamic hepatitis C virus genotypic and phenotypic changes in patients treated with the protease inhibitor telaprevir. *Gastroenterology*, **132**, 1767–1777.
38. Owsianka, A. M., Timms, J. M., Tarr, A. W., Brown, R. J., Hickling, T. P., Szwejk, A. *et al.* (2006). Identification of conserved residues in the E2 envelope glycoprotein of the hepatitis C virus that are critical for CD81 binding. *J. Virol.* **80**, 8695–8704.
39. Owsianka, A. M., Tarr, A. W., Keck, Z. Y., Li, T. K., Witteveldt, J., Adair, R. *et al.* (2008). Broadly neutralizing human monoclonal antibodies to the hepatitis C virus E2 glycoprotein. *J. Gen. Virol.* **89**, 653–659.
40. Wei, X., Decker, J. M., Wang, S., Hui, H., Kappes, J. C., Wu, X. *et al.* (2003). Antibody neutralization and escape by HIV-1. *Nature*, **422**, 307–312.

41. Zhang, M., Gaschen, B., Blay, W., Foley, B., Haigwood, N., Kuiken, C. & Korber, B. (2004). Tracking global patterns of N-linked glycosylation site variation in highly variable viral glycoproteins: HIV, SIV, and HCV envelopes and influenza hemagglutinin. *Glycobiology*, **14**, 1229–1246.
42. Utachee, P., Nakamura, S., Isarangkura-Na-Ayuthaya, P., Tokunaga, K., Sawanpanyalert, P., Ikuta, K. *et al.* (2010). Two N-linked glycosylation sites in the V2 and C2 regions of human immunodeficiency virus type 1 CRF01_AE envelope glycoprotein gp120 regulate viral neutralization susceptibility to the human monoclonal antibody specific for the CD4 binding domain. *J. Virol.* **84**, 4311–4320.
43. Pikora, C. A. (2004). Glycosylation of the ENV spike of primate immunodeficiency viruses and antibody neutralization. *Curr. HIV Res.* **2**, 243–254.
44. Moore, P. L., Gray, E. S., Wibmer, C. K., Bhiman, J. N., Nonyane, M., Sheward, D. J. *et al.* (2012). Evolution of an HIV glycan-dependent broadly neutralizing antibody epitope through immune escape. *Nat. Med.* **18**, 1688–1692.
45. Bukh, J., Thimme, R., Meunier, J. C., Faulk, K., Spangenberg, H. C., Chang, K. M. *et al.* (2008). Previously infected chimpanzees are not consistently protected against reinfection or persistent infection after reexposure to the identical hepatitis C virus strain. *J. Virol.* **82**, 8183–8195.
46. Gordon, D. F., Chung, R. T., Curry, M. P., Schiano, T. D., Emre, S., Babcock, G. J. *et al.* (2011). *Monoclonal antibody MBL-HCV1 suppresses return of HCV following liver transplantation.* The Liver Meeting, San Francisco, CA.
47. Herweijer, H. & Wolff, J. A. (2003). Progress and prospects: naked DNA gene transfer and therapy. *Gene Ther.* **10**, 453–458.
48. Liu, F., Song, Y. & Liu, D. (1999). Hydrodynamics-based transfection in animals by systemic administration of plasmid DNA. *Gene Ther.* **6**, 1258–1266.
49. Zhang, G., Budker, V. & Wolff, J. A. (1999). High levels of foreign gene expression in hepatocytes after tail vein injections of naked plasmid DNA. *Hum. Gene Ther.* **10**, 1735–1737.
50. Gadgil, H. S., Bondarenko, P. V., Pipes, G. D., Dillon, T. M., Banks, D., Abel, J. *et al.* (2006). Identification of cysteinylation of a free cysteine in the Fab region of a recombinant monoclonal IgG1 antibody using Lys-C limited proteolysis coupled with LC/MS analysis. *Anal. Biochem.* **355**, 165–174.
51. Kapadia, S. B., Barth, H., Baumert, T., McKeating, J. A. & Chisari, F. V. (2007). Initiation of hepatitis C virus infection is dependent on cholesterol and cooperativity between CD81 and scavenger receptor B type I. *J. Virol.* **81**, 374–383.
52. Kapadia, S. B. & Chisari, F. V. (2005). Hepatitis C virus RNA replication is regulated by host geranylgeranylation and fatty acids. *Proc. Natl Acad. Sci. USA*, **102**, 2561–2566.
53. Zhong, J., Gastaminza, P., Cheng, G., Kapadia, S., Kato, T., Burton, D. R. *et al.* (2005). Robust hepatitis C virus infection *in vitro*. *Proc. Natl Acad. Sci. USA*, **102**, 9294–9299.
54. Diao, J., Pantua, H., Ngu, H., Komuves, L., Diehl, L., Schaefer, G. & Kapadia, S. B. (2012). Hepatitis C virus induces epidermal growth factor receptor activation via CD81 binding for viral internalization and entry. *J. Virol.* **86**, 10935–10949.
55. Lindenbach, B. D., Evans, M. J., Syder, A. J., Wolk, B., Tellinghuisen, T. L., Liu, C. C. *et al.* (2005). Complete replication of hepatitis C virus in cell culture. *Science*, **309**, 623–626.
56. Paborsky, L. R., Fendly, B. M., Fisher, K. L., Lawn, R. M., Marks, B. J., McCray, G. *et al.* (1990). Mammalian cell transient expression of tissue factor for the production of antigen. *Protein Eng.* **3**, 547–553.
57. Hotzel, I., Chiang, V., Diao, J., Pantua, H., Maun, H. R. & Kapadia, S. B. (2011). Efficient production of antibodies against a mammalian integral membrane protein by phage display. *Protein Eng., Des. Sel.* **24**, 679–689.
58. Livak, K. J. & Schmittgen, T. D. (2001). Analysis of relative gene expression data using real-time quantitative PCR and the $2^{-\Delta\Delta C}{}_{T}$ method. *Methods*, **25**, 402–408.
59. Otwinowski, Z. & Minor, W. (1997). Processing of X-ray diffraction data collected in oscillation mode. *Methods Enzymol.* **276**, 307–326.
60. McCoy, A. J., Grosse-Kunstleve, R. W., Adams, P. D., Winn, M. D., Storoni, L. C. & Read, R. J. (2007). Phaser crystallographic software. *J. Appl. Crystallogr.* **40**, 658–674.
61. Emsley, P., Lohkamp, B., Scott, W. G. & Cowtan, K. (2010). Features and development of Coot. *Acta Crystallogr., Sect. D: Biol. Crystallogr.* **66**, 486–501.
62. Adams, P. D., Afonine, P. V., Bunkoczi, G., Chen, V. B., Davis, I. W., Echols, N. *et al.* (2010). PHENIX: a comprehensive Python-based system for macromolecular structure solution. *Acta Crystallogr., Sect. D: Biol. Crystallogr.* **66**, 213–221.
63. Murshudov, G. N., Vagin, A. A. & Dodson, E. J. (1997). Refinement of macromolecular structures by the maximum-likelihood method. *Acta Crystallogr., Sect. D: Biol. Crystallogr.* **53**, 240–255.